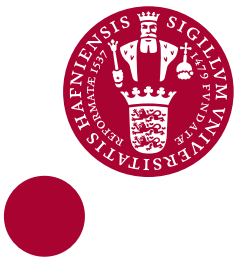

Point clouds from oblique stereo-imagery

two outcrop case studies across scales and accessibility

Vest Sørensen, Erik; Pedersen, Asger Ken; García-Sellés, David; Nykjær-Strunck, Max

Published in:
European Journal of Remote Sensing

DOI:
10.5721/EuJRS20154833

Publication date:
2015

Document version
Publisher's PDF, also known as Version of record

European Journal of Remote Sensing - 2015, 48: 593-614
doi: 10.5721/EuJRS20154833
Received 10/11/2014, accepted 20/07/2015

European Journal of Remote Sensing
An official journal of the Italian Society of Remote Sensing

www.aitjournal.com

Point clouds from oblique stereo-imagery: Two outcrop case studies across scales and accessibility

Erik Vest Sørensen[1]*, Asger Ken Pedersen[1,2], David García-Sellés[3] and Max Nykjær Strunck[1,4]

[1]Geological Survey of Denmark and Greenland, Øster Voldgade 10, DK-1350 Copenhagen K, Denmark
[2]Natural History Museum of Denmark, Øster Voldgade 5-7, DK-1350 Copenhagen K, Denmark
[3]Institut de Recerca Geomodels, Department de Geodinàmica i Geofisica, Facultat de Geología, Universitat de Barcelona, Martí i Franquès s/n, 08028 Barcelona, Spain
[4]COWI, Parallelvej 2, 2800 Kongens Lyngby, Denmark
*Corresponding author, e-mail address: evs@geus.dk

Abstract

Digital elevation models (DEM) were generated from oblique stereo-images acquired with a handheld digital camera. Two model scenarios are considered. Firstly, at local outcrop scale, with easy access, and distances between camera and outcrop varying between c. 40 m and c. 120 m, a very dense and high resolution point cloud was produced. The quality of the point cloud was evaluated against a terrestrial laser scan derived model of the same outcrop. The deviation between the two datasets varies between 0.02 m and 0.09. This is negligible for most geological purposes and illustrates the potential of using terrestrial photogrammetry at local outcrop scale as an alternative to lidar generated elevation data. Secondly, the method is explored at a regional scale, where a set of oblique stereo-images of a remotely located steep inaccessible mountain cliff was collected from a helicopter at a distance of c. 2-5 km under challenging and unfavourable conditions. The quality of the point cloud was evaluated against two elevation models extracted from conventional aerial photographs. Compared to a DEM extracted from monochrome aerial photographs, such as are often the only available topographic source for remote regions, a clear improvement in resolution is observed. Comparison with a DEM extracted from high resolution coloured aerial photographs shows the two digital elevation models to be very similar in resolution and with root mean square deviation (RMSE of 6.0 m).

Keywords: Point cloud, photogrammetry, digital elevation model, handheld camera, remote, outcrop.

Introduction

Visualisation of geological outcrop data in so-called Digital Outcrop Models (DOM) is gaining importance and popularity within the field of geology [Bellian et al., 2005]. In a DOM, geological data (geological boundaries, bedding, faults etc.) is presented within a virtual environment that can be rotated in three dimensional space and used for geological

interpretation [Bellian et al., 2005].
DOMs have found particular use in the fields of reservoir studies [Pringle et al., 2004; Enge et al., 2007; Janson et al., 2007; Rotevatn et al., 2009; Fabuel-Perez et al., 2010], structural studies [Ahlgren and Holmlund, 2003; Sagy et al., 2007; Olariu et al., 2008] and in cliff erosion and natural hazards studies [Lim et al., 2005; Rosser et al., 2005; Jaboyedoff et al., 2007; Kuhn and Prüfer, 2014] as well as in the generation of virtual field trips [McCaffrey et al., 2010].
Central to the generation of a DOM is the digital elevation model that describes the morphology of the outcrop. Such a model is most times generated using a ground-based Terrestrial Laser Scanner (TLS) [Bellian et al., 2005; Buckley et al., 2008a; Buckley et al., 2010] but could equally well be supplied by other means such as for example photogrammetry.
Development within the digital camera industry with increased image sensor resolution as well as software, both within traditional softcopy photogrammetry and in the emerging fields of structure from motion (SfM) [Lowe, 2004; Snavely et al., 2008; Fonstad et al., 2013], and the combination with dense stereo matching from Multi View Stereo (MVS) [Hirschmüller, 2005; James and Robson, 2012; Favalli et al., 2012], has made image-based semi-automatic terrain model extraction from oblique images within the geoscience field highly feasible.
In this study we would like to explore a more classical photogrammetric approach developed for three-dimensional geological and structural analysis of outcrops, originally termed multi-model photogrammetry (MMP) [Dueholm, 1992]. In multi-model photogrammetry, oblique stereo images obtained with small-frame cameras are combined with triangulated aerial photographs traditionally used for topographic and geologic mapping. It is a versatile method that combines stereo-models at varying scales and viewing angles into a network of stereoscopic models from which three dimensional geological data can be manually extracted. MMP differs from the DOM approach in that normally only the three dimensional features (geological boundaries, faults etc.) are extracted stereoscopically and no DTM as such is produced. Such DTM can however also be extracted from the oblique images as an alternative to for example TLS data. Because only a camera, that can be handheld or mounted on a tripod, is needed during fieldwork, the method is very portable and highly suited for use in for example a helicopter, small airplane or a boat. In this way MMP extends in range of use from metre scale [Garde, 1992a; Vosgerau et al., 2010], to kilometre scale [Garde, 1992b; Pedersen and Dueholm, 1992; Dueholm and Olsen, 1993; Pedersen et al., 1998; Pedersen et al., 2002; Pedersen et al., 2006] or even hundreds of kilometres [Pedersen et al., 2006 and references therein]. This is at least an order of magnitude larger than the typical operational extent using TLS. This makes terrestrial photogrammetry from oblique images interesting, both in terms of 3D-mapping but also as a means of generating digital elevation models that could serve as surface data in for example a DOM.
The recent combined SfM and MVS approaches by James and Robson [2012] are in many ways similar to MMP, in that stereo-images are acquired at different scales and from different viewing angles. However, with SfM and MVS, images are acquired with a much larger overlap and from a more divergent set of imaging positions [James and Robson, 2012] than in the traditional MMP setup which typical involves one or two parallel flight lines (overview and close-up). The obvious advantage of the SfM and MVS approach is

that a more complete coverage of the outcrop is obtained with less occlusion zones than obtained when only using single stereo-lines. However, this also restricts the usage to locations where the nature of the outcrops allows them to be photographed from many different positions. In many quarries, sea cliffs and inaccessible mountain areas this is not practically feasible unless involving some kind of manned or unmanned aircraft. In such cases, traditional oblique photogrammetry from stereo-pairs or single blocks of stereo-images with continuous stereo-overlap, now used for decades, may still be highly relevant.

In this study, we report on the use of oblique stereo-images acquired with handheld digital consumer cameras to generate outcrop elevation models using a classical photogrammetric approach. Two outcrops at different scales and with different accessibility are considered to study how the cameras perform in different conditions. The first case exemplifies an outcrop with easy access at a local scale (200 m) and involves stereo-images collected from close range (40-120 m) while walking on foot and under optimal conditions. The quality of the produced terrain model is here evaluated against a TLS model of the same outcrop. The second case exemplifies a partly inaccessible outcrop in a remote setting at a more regional scale (12 km) and involves stereo-images collected from a greater distance (2-5 km) using a helicopter and a handheld camera under more challenging and unfavourable conditions. The data are here compared to DEMs extracted from conventional vertical aerial photographs which are considered the best available topographic data from the area.

Field areas and methods

Faxe Quarry, Denmark

A small area within the south-eastern corner of the Faxe Quarry, Denmark (Fig. 1) was chosen as test site for the comparison between oblique terrestrial photogrammetry and TLS at a local scale with easy access. The quarry, which is being actively quarried, is approximately 1 km^2 in size, 45 m deep and consists of Lower Paleocene (middle Danian), bryozoan and coral limestone [Asgaard, 1968; Floris, 1980; Bernecker and Weidlich, 1990]. An Optech ILRIS-3D laser scanner was deployed during the experiment and the outcrop was scanned from multiple positions (Fig. 1) to cover the lateral extent of the outcrop (c. 200 m). Distance from the scanning position to the outcrop varied between 40 and 120 m depending on access, and scan positions were registered with a consumer grade GPS using differential EGNOS corrections. This gives a positional error around 3 m.

The photogrammetric survey was conducted using a handheld Canon EOS 1Ds MARKIII 21 megapixel (5616 x 3744) digital Single Lens Reflex (SLR) camera fitted with a fixed canon 35 mm lens (Canon EF 35mm f/1.4 L USM) and a BW UV-filter. The image sensor pixel size of the camera was 6.4 µm and camera and lens were calibrated before the test using a theodolite surveyed steel grid with around 100 targets [Dueholm, 1992]. The lens was focused and locked at infinity during calibration and the field test. The result of the calibration is given in Table 1. Images were shot on foot from the bottom of the quarry, walking in straight lines parallel to the surface of interest and from approximately the same distance as the laser scans (photo acquisition scale 1:1400-1:3400). Stereo overlap was approximately 80 % and the camera positions in relation to the scan positions are shown in Figure 1. A total of 15 images were taken of the outcrop as illustrated in the figure, and examples of the appearance of the outcrop are shown in Figure 2.

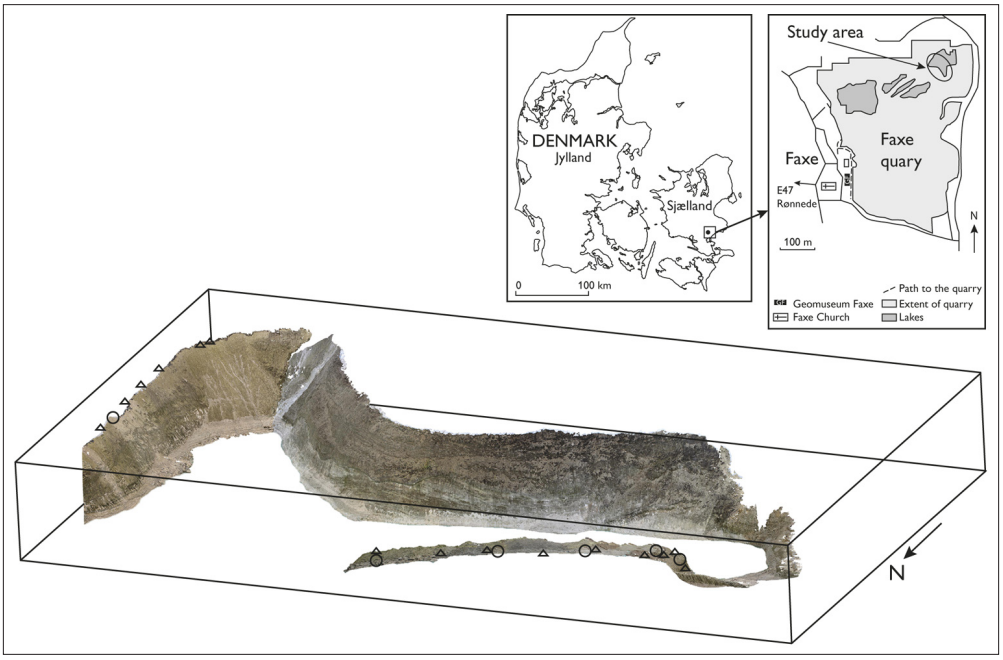

Figure 1 - Overview figure showing the investigated outcrop within the Faxe Quarry as an RGB coloured point cloud. Insets show the location of the quarry. The dimension of the outcrop is given by the bounding box that measures 220 x 133 x 28 m. Scan- and camera positions are indicated with black circles and triangles respectively. The outcrop was covered by 15 TLS scenes acquired from 6 different positions, while a total of 15 images were collected from the outcrop as indicated on the figure.

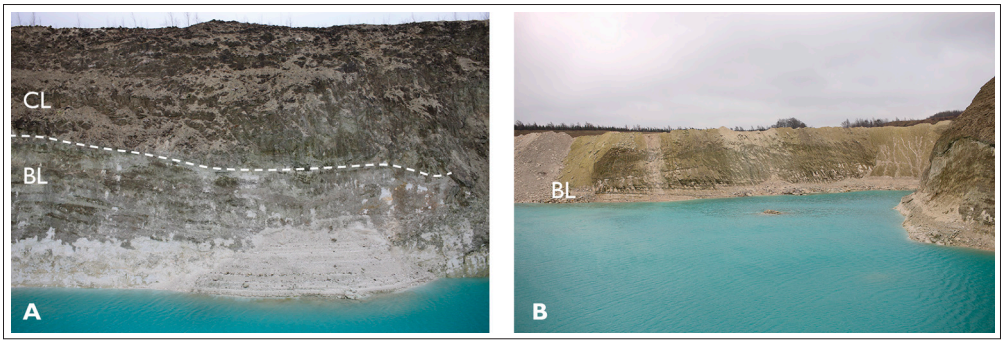

Figure 2 - Examples of the images used in the experiment. a) Image showing the appearance of the outcrop at close range from a distance of c. 40 m. The outcrop is made up of Bryozoan limestone (BL) with thin flint layers that makes up the lower part of the outcrop, and Coral limestone (CL) that forms the upper part. Field of view is c. 22 m and the height of the outcrop is c. 22 m. Variation in depth across the image is around 20 m. b) Image showing the appearance of the outcrop from a distance of c. 120 m. Field of view around 100 m and height around 16 m. Variation in depth from the lower to the upper part of the outcrop is around 16 m.

Digital terrain models were extracted from the images after returning from the field using a photogrammetric workstation running the commercial photogrammetric mapping and geospatial analysis software package SocetSet v5.6 and SocetGXP 3.1 from BAE Systems, and applying a classical photogrammetric workflow. First step was triangulation of the stereo images into a relative stereo-block using tie-points measured manually within SocetSet. The process of manual tie-point measurement could be automated using automatic tie-point measurement routines within the software. However, because of the small amount of stereo-images it was found faster to measure them manually. In addition a few points along the shoreline were also measured for levelling purposes. The commercial Bingo-F bundle block adjustment software was used to do the triangulation. The uncertainty of the bundle block adjustment amounts to around 2 μm, roughly 1/3 of the pixel size (6.4 μm) and is within the expected. Control points for transforming the relative stereo models into the coordinate system of the laser-scanner models were derived from manual recognition of common points between the laser-scan models and the stereo-models. Bingo-F bundle block adjustment software was used during this step using a 7-parametre Helmert transformation, and the calculated error amounts to around 0.05 m. Finally, the extraction of terrain elevation was undertaken using the NGATE automatic terrain extraction module residing within SocetGXP [BAE systems, 2007]. NGATE performs an image and edge correlation routine on every pixel (described in SocetSet and SocetGXP user manuals). However, in order to get NGATE to perform properly, the bundle adjustment solution of the first step was used for the terrain extraction. The reason for this is that the sensor model used within SocetSet has been designed to work with conventional vertical aerial photographs. The terrain model was then subsequently transferred from image-space into ground space using the previously established results of the Helmert transformation.

Disko, Greenland

A 12 km north facing-cliff section on northern Disko, Central West Greenland was selected as an example of an outcrop on a more regional scale with difficult access (Fig. 3). The outcrop is a steep mountain face consisting of a succession of Paleocene lava flows [Larsen and Pedersen, 2009] erupted within the Nuussuaq basin. It is located 150 km from the nearest major town and can be reached by boat or helicopter. Within the area, fjords and deeply incised valleys with up to 2000 m of relief offer excellent seismic-section sized exposures of the three-dimensional architecture of the basin [Pedersen et al., 2006; Dam et al., 2009]. This makes it an excellent test site for point cloud extraction from oblique images at a more regional scale.

The area is covered by two different sets of conventional aerial photographs. The oldest set consists of monochrome vertical aerial photographs (1:150.000) collected in 1985. The newest set consists of higher resolution RGB-coloured aerial photographs collected in 2009, covering parts of the study area (Fig. 3, respectively the right and left parts). The coloured aerial photographs have a ground sampling distance (GSD) of around 0.5 m and their orientation is based on triangulation of inertial GPS data while the black and white aerial photographs have been oriented by traditional ground point surveying.

Digital highly oblique stereo-images were acquired in 2012 using a handheld Canon EOS 5Ds MarkII 21 megapixel (5616 x 3744) digital (SLR) camera fitted with a fixed canon 35 mm lens (Canon EF 35mm f/1.4 L USM) and a BW UV-filter. The camera system

was calibrated beforehand using a similar approach as described above. The result of the calibration is given in Table 1.

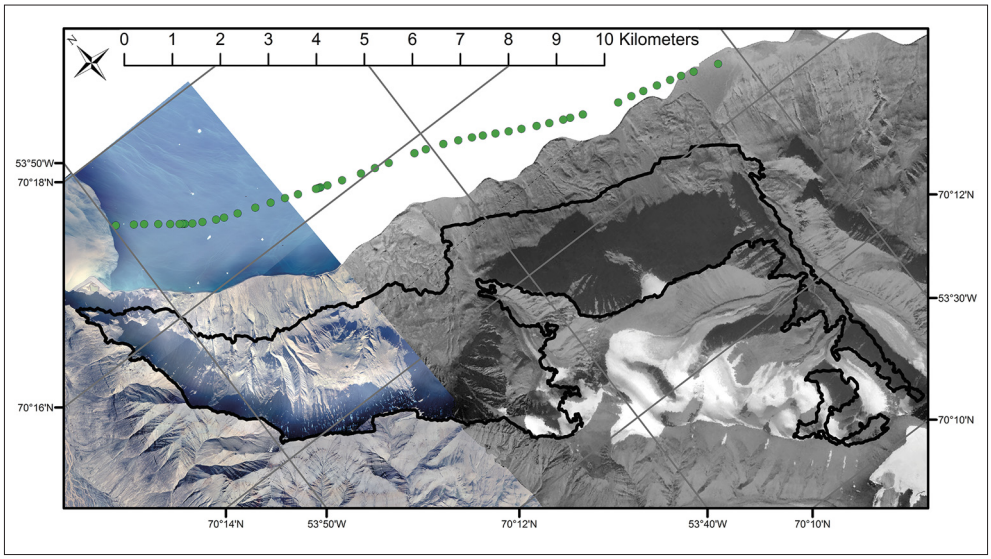

Figure 3 - Overview figure of the Disko study area. Small inset with a red dot shows the location of the study site in West Greenland. The area is partly covered by coloured aerial photographs (left hand side) and a set of older black and white aerial photographs in the right hand side of the figure. Green dots show the location of the oblique images taken with a handheld digital camera from a helicopter. Black polygon indicates the location of the cliff section covered by oblique stereo-imagery. Note that the steep N-NE facing slopes generally is covered in shadows.

The images were taken through an open window in a helicopter using a shutter speed of minimum 1/250 second during photographing in order to minimize image blur due to helicopter vibrations and relative movement between the helicopter and the outcrop during exposure. The pilot was instructed to fly parallel to the cliff and the camera was pointed approximately perpendicular to the slope of the cliff with a distance to the cliff of around 2-5 km. The images were taken with the purpose of stereoscopic photo interpretation and were collected during a geological reconnaissance flight. The data set consists of 120 km of close to continuous highly oblique stereo images. A small subset (51 images) of the data, was selected for the purpose of this paper. Examples of the outcrop are given in figure 4. The images in the subset were collected during 6 min of flying time while the entire dataset were collected within 1 hour of flying. The oblique images were imported and oriented within SocetSet following a similar approach as described above. However, because of the larger number of images involved, an automatic tie measurement routine was deployed during the triangulation. Error on the relative triangulation in image space amounts to around 2 µm. Aerial photographs (monochrome and RGB-coloured) were used as control point source, and control points were collected manually. The accuracy of the triangulation, as given by the root mean square deviation (RMSE) amounts to around 5 m. The procedure for the terrain extraction was as described for the Faxe Quarry.

Table 1 - The camera systems were calibrated before being deployed in the field using a steel grid with around 100 marked points (located at the Technical University of Denmark [Dueholm, 1992]). The result of the calibration is given as distortion pairs. The accuracy of the calibration is approximately 1/3 pixel.

		Radius in mm																	
		0	1.3	2.6	3.9	5.2	6.5	7.8	9.1	10.4	11.7	13	14.3	15.6	16.9	18.2	19.5	20.8	22.1	23.4
Lens distortion in microns	Canon EOS 1D MarkIII	0	0	-1	-5	-11	-22	-37	-57	-82	-113	-150	-190	-234	-281	-327	-371	-411	-441	-459
	Canon EOS 5D MarkII	0	0	-1	-4	-9	-19	-34	-54	-79	-111	-149	-191	-236	-284	-328	-369	-402	-419	-418

	Focal length (mm)	Principle point displacement (mm)	
		x	y
Canon EOS 1D MarkIII	34.326	-0.053	0.294
Canon EOS 5D MarkII	34.310	0.007	0.303

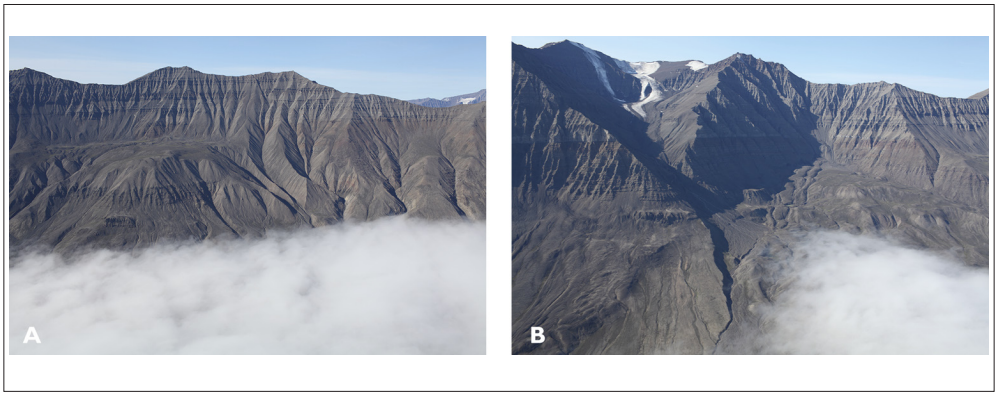

Figure 4 - Photographs showing the outcrop as seen from around 4 km distance. The outcrop consists of gently dipping Paleocene lavas that overlie Cretaceous sediments (below cloud cover). The images were taken using a handheld digital camera while flying approximately parallel to the cliff. a) Example of a well exposed an evenly illuminated part of the outcrop. Field of view is approximately 3000 m and the visible vertical relief is around 1200 m. Cloud base is at 200 m above sea level and the peak in the central part of the image reaches 1410 m. b) Example of part of the outcrop where the NW facing cliff faces are partly in shadows. Field of view is approximately 3900 m and the vertical relief is around 1600 m. The peak in the central part reaches 1700 m.

Results

Faxe Quarry

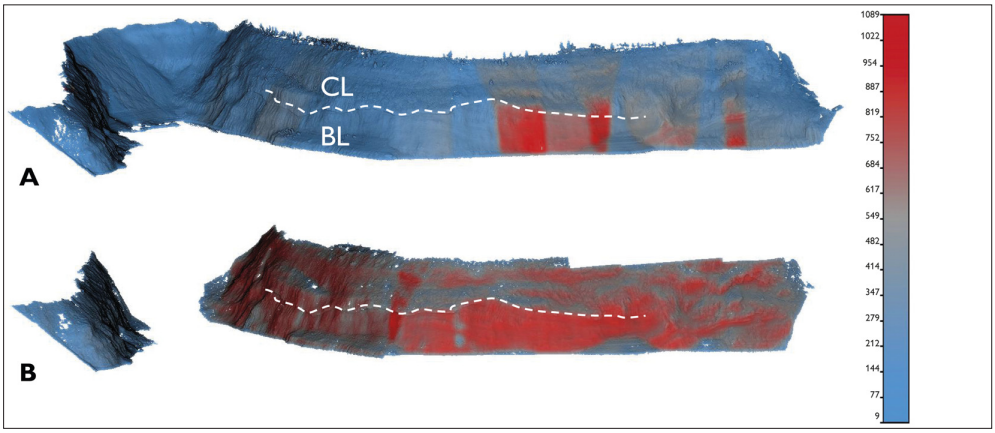

Figure 5 - Results of the Faxe Quarry test study. a) Perspective view showing the point density of TLS point cloud coloured according to density. Size of the scene is approximately 200x110x28 m. There is generally an even distribution of point density throughout the dataset. However, in places, sharp boundaries in point density are observed. These correspond to the overlapping areas between individual scans. The point density is calculated as the number of points within a sphere with 1 m radius divided by the volume of the sphere. b) Perspective view showing the point density of the photogrammetry derived point cloud data. The density was calculated as for Figure 5a. Photogrammetry derived data generally has a higher point density than the TLS data.

The point cloud produced using TLS consist of around 9 M points (Fig. 5a) describing the topography of the outcrop, while the point cloud derived using photogrammetric techniques contains around 21 M points that only partly cover the outcrop (Fig. 5b).

The TLS derived point cloud is spatially well distributed throughout the area with an average nearest neighbour distance of 0.02 m and point density varying from around 100 points/m^2 to an upper limit of around 1000 points/m^2 as illustrated in figure 5a. Sharp boundaries, or contrast, in point densities do however exists in the TLS data, reflecting boundaries between overlapping scans (Fig. 5a). Photogrammetry derived data (Fig. 5b) is also spatially well distributed with an average nearest neighbour distance of c. 0.014 m - 0.022 depending on distance to the outcrop. The point density (Fig. 5b) is generally higher for the photogrammetry derived data with densities varying between a few hundred to around 1000 points/m^2). The difference is somewhat arbitrary and to some extent reflects how the laser scanner was set up. The point clouds were compared using the open source software Cloud Compare (http://www.danielgm.net/cc/). We used an automatic best fit alignment routine (Iterative Closest Point (ICP); [Besl and Mackay, 1992]) within the software to determine a best fit between the two data sets. During the alignment process we assumed that the TLS derived data were of superior accuracy to the photogrammetrically derived model, and the TLS data was therefore kept fixed during the alignment. The result of the ICP adjustment is given in table 2 and is a measure of how well the ground control solution performed to match the lidar bench mark dataset. The RMS error on the ICP transformation amounts to 0.03 m and is comparable with the error on the ground control picking (RMS = 0.05). Judging

from the adjustment matrix (Tab. 2), only small angular correction is gained from the ICP alignment. The deviation between the two datasets was subsequently calculated using the M3C2 plug-in for CloudCompare, which gives the deviation between the data sets as signed distances [Lague et al., 2013]. The result are shown in Figure 6 and summarized in Table 2.

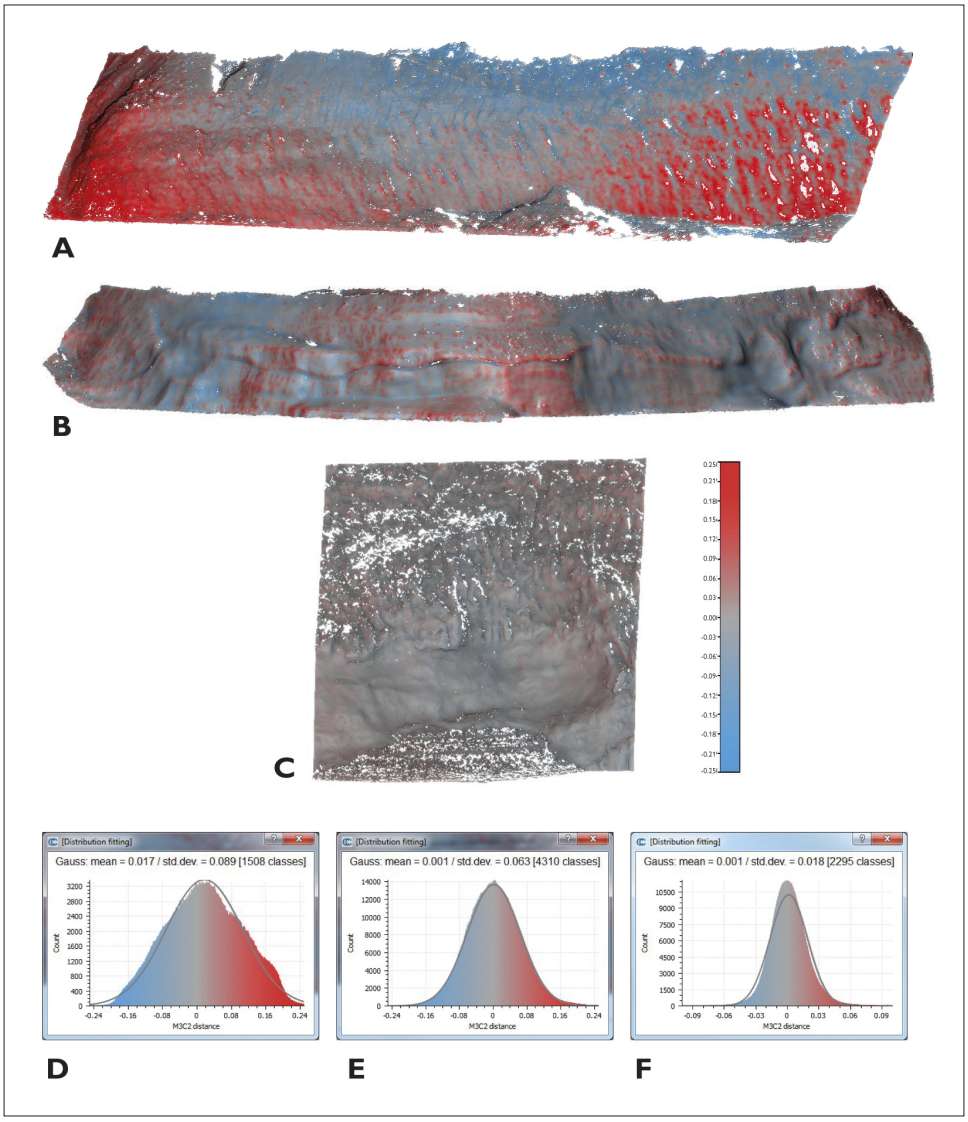

Figure 6 - Comparison figure showing the difference between TLS and photogrammetry derived elevation data. a) Perspective view at photo scale 1:3400. Characteristic oblique streaks reflects relief features produced by an excavator spade. Size of the scene is approximately 77x31x18 m. b) Perspective view at photo scale of 1:1400. Size of the scene is approximately 153x85x25 m. c) Perspective view showing comparison between a single stereo model derive point cloud (photo scale 1:1400) and the corresponding TLS scene. d-e) Histogram plots of the standard deviation for Figure 6a, b and c. The deviation generally follows bell-shape Gaussian curves. See text for discussion.

Table 2 - Table summarizing survey parameters and results from the Faxe Quarry and Disko case study areas. GSD is the ground sampling distance or ground pixel size. Data from Faxe was evaluated against TLS data of the same outcrop. The 4x4 rotational matrix comes from fitting of the photogrammetry data to the TLS data using a ICP routine within Cloud Compare. Point density is calculated as the number of points within a sphere with a 1 m radius divided by the volume of the sphere Data from Disko was evaluated by DEM comparison of the 5 m DEM´s produced form conventional coloured aerial photographs and oblique stereo-images. Point density is calculated as the number of points within a sphere with a 1 m radius divided by the volume of the sphere.

	Faxe		Disko
	Terrestrial laser scanner	**Oblique stereo-images**	**Oblique stereo-images**
Distance to outcrop	40-120 m	40-120 m	2-5 km
Photo acquisition scale		c. 1:1400 - 1:3400	
Number of points in point cloud	9 M	21 M	31 M
Ground sampling distance (pixel size)		0.006-0.02 m	0.4-0.9 m
Quoted manufacture accuaracy	7 mm from 100 m distance		
Error on registration	3 m		
Error on triangulation in image space (RMS)		2 µm (1/3 the pixel size)	2 µm (1/3 the pixel size)
Absolute accuaracy (RMS) from control points		0.05 m	5 m
Iterative closests point (ICP)	1.002 0.004 0.002 -27.31		
4x4 rotational matrix	-0.004 1.002 0.003 28.705		
(RMS = 0.03)	-0.002 -0.003 1.002 26.958		
	0 0 0 1		
Average nearest neighbour	0.02 m	0.014 m	0.8 m
Point density	100-1000 points/m^2	100-1000 points/m^2	0.1-0.4 points/m^2
Point cloud deviation (optimal)		0.02 - 0.09 m	
Relative precision ratio (optimal) (deviation/distance to outcrop)		0.06 - 0.08 % (40 - 120 m)	
Point cloud deviation (combined model)		0.06 m (0.15%)	
Deviation (DEM comparison - RMS)			6.0 m

Disko

The photogrammetry derived point cloud produced from the highly oblique images taken from a helicopter consists of 31 M points (Fig. 7) describing the rugged terrain of the north side of Disko.

Points are generally evenly distributed in areas with optimal viewing angles (right angles to the topography) and low amounts of shadows. However some areas gave poorer results. These areas correspond to areas where the cliff is either oriented at oblique or low angles

to the observational direction of the camera or to areas that are within shadows (Fig. 4b and Fig. 7). This gives large variations in depth (hundreds of metres to kilometres). Furthermore, one area, which is a partly hidden gully, also has poor stereo coverage (Fig. 7). The data set has an average nearest neighbor distance of 0.8 m while the point density varies between 0.1-0.4 points/m^2). The data is here evaluated against topographic data extracted from conventional aerial photographs, both qualitatively and quantitatively. The results are shown in figure 8 and summarized in Table 2.

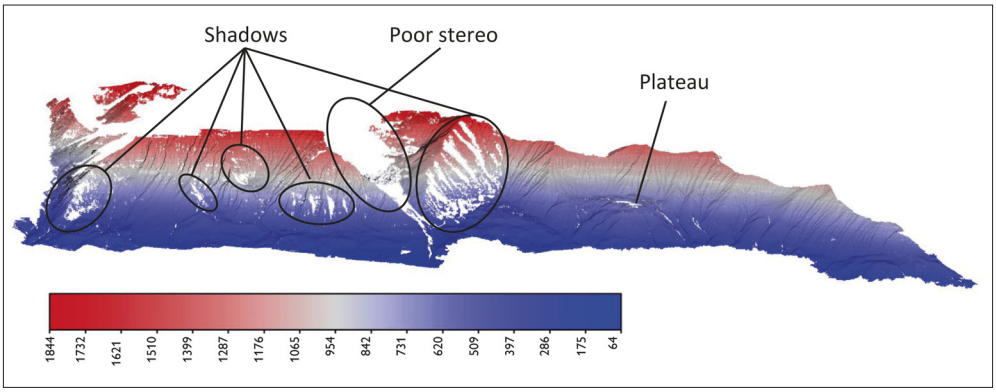

Figure 7 - Figure showing the point cloud produced from the oblique images in perspective view from north towards south. The point cloud is coloured according to height and colour scale is given in the figure. Points are generally evenly spaced throughout the outcrop. However, certain areas have a less dense coverage. These are typical NW facing cliff faces that are within shadows or in combination with poor stereo coverage. Furthermore, a low observation angle with respect to the terrain results in less coverage for plateau areas. Finally, large variation in depth (5 km) in the valley in the eastern part (left part) of the area generally gave poorer results.

Discussion

Close range: Faxe Quarry

Comparison between DEM´s derived by photogrammetry and laser scanning

Using terrestrial oblique stereo images for DEM extraction within the geosciences field has previously been applied successfully [Chandler et al., 2002; James et al., 2006; James et al., 2007; Haneberg, 2008; Gessner et al., 2009; Sturzenegger and Stead, 2009] and is as such not a new topic. The results of our experiment, in accordance with previous studies, show that the use of high-resolution handheld digital cameras and photogrammetric methods is a method capable of producing elevation models of geological outcrops with high resolution. This is especially true in the close range case, where comparison with the TLS derived model shows the two data sets to be very similar.

For the photogrammetric approach the source of error is mainly related to the calibration of the camera system (estimation of principal point, focal length and lens distortion) and the imaging settings (shooting distance, baseline, camera intersection angle) whereas the accuracy of the terrestrial laser scanner consist of a range of components such as the angular accuracy, range accuracy, resolution setting, edge effects, surface reflectivity which all are manufacture dependent (7 mm from 100 m distance). The measurement accuracy do in

the photogrammetric setup amounts to c. 2-7 mm (1/3 pixel), while the accuracy in depth, which is determined as the product of the measurement accuracy, image scale and the ratio between distance to the object and the image baseline (distance between camera positions), varies between 0.01-0.03 m. In addition, an error contribution of 1/3 pixel from the camera calibration should also be considered. However, because NGATE performs a pixel-wise matching and only single stereo-model matching is being utilized; the GSD of the images essentially determines the accuracy of the undertaken photogrammetric approach.
The deviation between the two datasets varies across the outcrop according to distance, as would be expected. For the long range part of the outcrop (Fig. 6a) surveyed from a distance of c. 120 m (single stereo pair at photo scale 1:3400) the deviation amounts to c. 0.09 m which gives a relative precision ratio (average deviation in relation to the distance to the outcrop) of 0.08% while the deviation for the closer range (photo scale 1:1400) part of the outcrop (Fig. 6b) amounts to c. 0.06 m and a relative precision ratio of 0.15%. The deviation between the two datasets generally follows a bell-shape Gaussian curve (Fig. 6d, e and f). However, systematic errors are observed in parts of the outcrop in for example Fig. 6a where characteristic oblique streaks reflect relief features produced by an excavator spade. The deviation generally varies systematically across these features with positive values on the left hand side (side facing towards the camera) and negative values on the right side facing away from the camera. Furthermore, a certain degree of symmetry exists within the data, which is seen as a general tendency for positive values in the lower parts and towards the sides of the model (Fig. 6a) coupled with a tendency for negative values in the upper central part of the extracted model. In the closer range part of the outcrop (Fig. 6b) systematic errors are mostly seen as areas of predominantly either positive or negative deviation that are separated by rather sharp vertical boundaries. These are in many cases coincident with sharp contrasts in point density of the TLS data (Fig. 5a) and likely reflect small errors in the scan alignment. Furthermore a few hot-spot areas in the upper central part of Figure 6b reflect vegetation that is less well represented in the photogrammetry data. Comparing the point cloud derived from a single stereo-model with a single TLS scene allows for a better assessment of the difference between the methods at optimal conditions. In such case (Fig. 6c) the standard deviation drops to c. 0.02 m (relative error of 0.06%).
Despite the increasing deviation between the two datasets with distance, the produced point cloud is still very dense and detailed, and the magnitude of deviation is for most geological purposes insignificant across the scale investigated. The undulating boundary between bryozoan limestone and overlying coral limestone is for example seen equally well in both data sets (Fig. 5a and b). In this aspect it is important to emphasize that geological outcrop interpretation mostly relies on colour as well as geometric texture changes, which in the case of photogrammetry can both be derived directly from the images, ensuring a coherent dataset. In the case of TLS only a precise geometric point cloud is provided directly.

Conditions of data Acquisition

The present study was conducted in overcast weather and the outcrop had a uniform steep slope without abrupt major changes in scale/depth. This made the outcrop evenly illuminated and without shadows. Furthermore, the nature of the outcrop made it possible to point the camera approximately perpendicularly to the slope face in most areas, which gives the best results for both camera and laser scanner. The experiment was therefore

conducted under optimal conditions. At a different outcrop in a more complex landscape with higher relief and more change in scale/depth, a similar comparison is likely to give different results. Further testing would be beneficial to determine how the camera performs in different settings and conditions, as well as to provide a more complete examination of the accuracy of the two methods using independent control point sources. However, at a local scale and at close range, similar techniques can be deployed for georeferencing the models into absolute space. In principle, similar absolute positional accuracy should be obtainable using either method.

Speed of DTM generation

An important aspect and argument for using TLS is the rapid speed at which the terrain models are generated. However, we find the two techniques to be very similar in terms of the time involved. In the present study, TLS models (15 lidar scenes) of the entire outcrop were acquired and aligned within one working day. This is comparable in time to the setup of the stereo-images and subsequent extraction of the terrain models. In the given setup a total of 15 stereo-images were oriented manually within a working day to cover the outcrop, including the extraction of the terrain models (3 hours) and therefore compares to the TLS setup. The field acquisition time was considerably faster using photogrammetry. In the Faxe Quarry, the images could be collected in about 30 min, roughly equalling the time it took to acquire one TLS model from one scanning position. However, using a different scanner with a broader field of view (360°) would decrease the time needed for TLS data acquisition to around one hour and three scan positions, making the time spent in the field comparable for the two methods.

Evaluation

This simple field comparison is not a full evaluation of the two methods, which is beyond the scope of this paper. We consider that the methods are complementary and the matter of choice depends on the scope of the project. However, our comparison still demonstrates that the methods deliver similar results in terms of resolution. The single most important difference, as we see it, is that the simplicity of using just a handheld camera makes photogrammetry highly mobile. This makes photogrammetry from oblique images well suited for field-based outcrop studies both from ground observations and from moving operational platforms.

Long range: Disko

Conducting field work on a regional scale in remote mountaineous areas with near vertical and often inaccessible cliff exposures is challenging and relies on remotely sensed data combined with field observations. Traditional air- and space borne nadir-looking sensors are appropriate for regional structures but fail to resolve the finer details because of inappropriate field of view [Dueholm, 1992; Rittersbacher et al., 2013]. This makes photogrammetry from oblique images using handheld cameras interesting because it can be deployed from a helicopter or a small aircraft at an optimal viewing angle perpendicular to the slope of the outcrop without the need to modify the aircraft. This principle has been applied successfully in the large scale three-dimensional studies of the Nuussuaq Basin since the 1990´s.

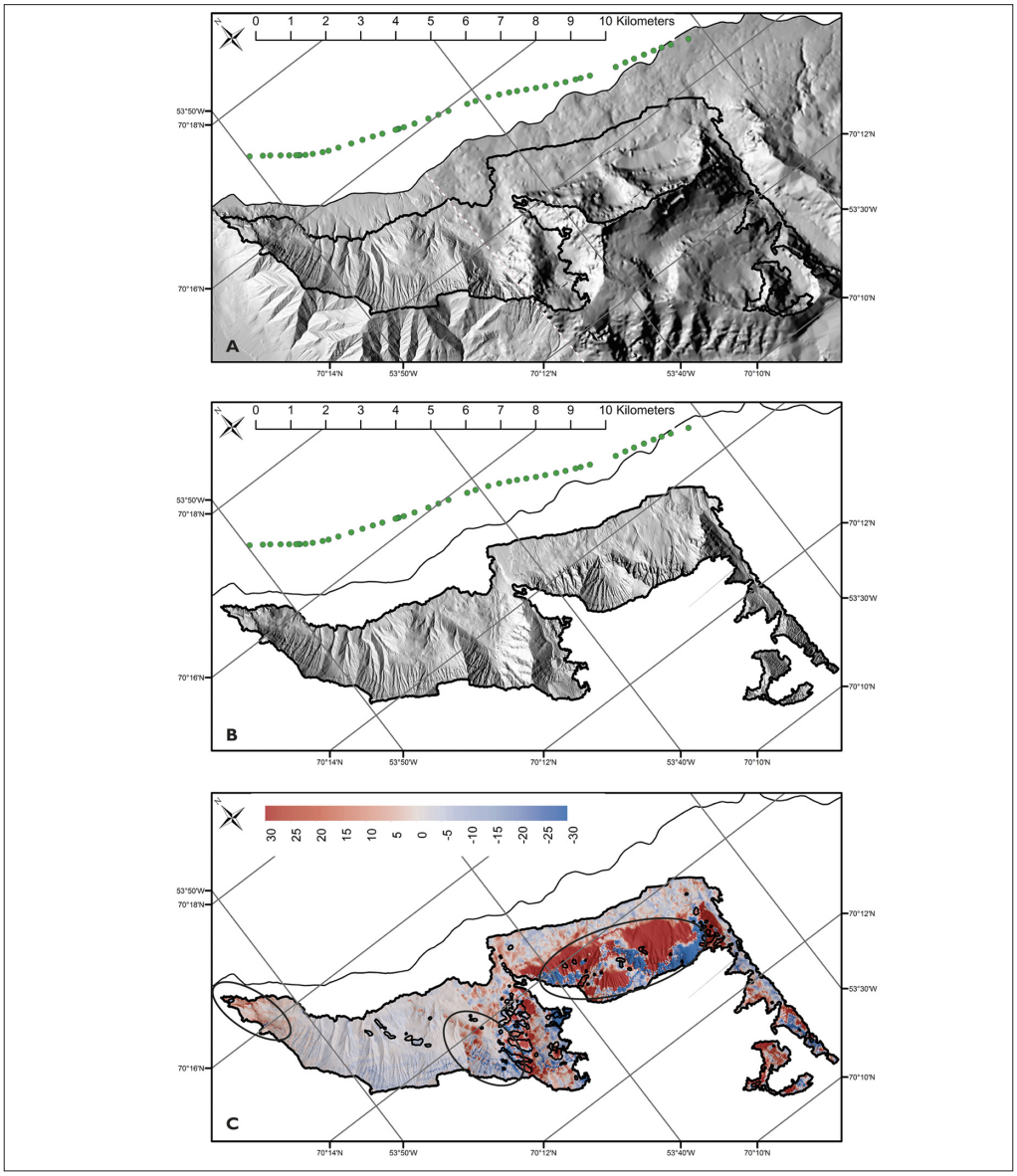

Figure 8 - Figure showing the digital elevation model extracted from oblique images in relation to existing topographic data. a) Shaded relief map of the DEM extracted from conventional aerial photographs. Left part (divided by white stippled line) is a 5 m DEM extracted from couloured aerial photographs while the right part is a 30 m DEM extracted from black and white aerial photographs. Black polygon indicates the location of DEM produced from the oblique images (Fig. 7). b) Shaded relief map of the 5 m DEM extracted from the oblique images. There is a clear improvement in resolution compared to the 30 m DEM while comparison with the 5 m DEM extracted from the coloured aerial photographs shows the two data sets to be very similar. Most ravines and gullies, plateaus as well as the "layer cake" stacking of the lava flows are seen equally well in both datasets. c) DEM-difference map shown upon a shaded relief map. Colour scale is given on the figure. Encircled areas corresponds to areas that are within shadows in the control data while small black polygons indicate areas of no-data from the oblique images.

An important aspect of geological field work in remote areas is to minimized flying time (helicopter and small aircrafts) to keep the operational expense at a minimum. This typically means that only selected key localities are surveyed in detail, while other areas are only observed from a distance when for example travelling between locations. This again brings in the camera handy because it can be deployed in such cases without increasing the travelling costs. Inspired by the close range comparison, we here explore how well the camera performs at longer range (2 - 5 km distance) in terms of extraction of elevation data.

Comparison with DEM´s extracted from vertical photographs

Judging from the specification of the camera, a distance of 2 - 5 km to the outcrop should give images with a pixel resolution on the ground in the 0.4-0.9 m range (image scale c. 1:57.000 - 1:143.000). The extracted point cloud was therefore expected to give results (in terms of resolution) roughly comparable to the DEM extracted from the coloured aerial photographs (GSD 0.5 m) partly covering the area. Visual comparison (Fig. 8a and 8b) shows that this is close to being the case. It also shows that by simply photographing the cliff walls while flying past them anyway, at little or no extra cost in data collection, a clear improvement in resolution compared to the 1:150.000 aerial photographs is gained. This was anticipated, and is important to emphasize, because in many remote areas such types of aerial photographs still provide the only available topographic data.

A more quantitative estimate of the quality of the produced point cloud is given by the comparison with a 5 m DEM extracted from the coloured aerial photographs. Here we observed an overall good fit between the two datasets (RMS = 6.0 m). However, considering the introduced interdependency by using control points obtained in the aerial photographs, this is not surprising. Inspection of Figure 8c shows that certain areas stand out as anomalous. Most notable are two broader areas (encircled) in the western and the central part of the study area. These areas correspond to parts of the outcrop that are within shadows in the RGB-coloured vertical aerial photographs (Fig. 3). A similar feature is seen in the comparison with the monochrome aerial photographs (Fig. 8c) where large areas are within shadows. At a finer scale, deviation to some extent correlates with terrain elements. This is for example seen as streaks along the central axis of gullies as well as streaks along the strike of some of the more prominent lava flows in the upper central part of the cliff section. In addition, certain areas are poorly portrayed (no data) in the extracted elevation data. These areas typically correspond to areas that are at an oblique angle to the camera, in shadows, or have poor stereo coverage (Fig. 8b and c). From a closer inspection of the camera positions, it is apparent that the images were not acquired precisely perpendicular to the terrain although originally intended to be so. This is probably a consequence of lacking adjustment of camera height (helicopter altitude) to the changing topographic relief during the over 120 km long oblique stereo-line.To summarize, this study was conducted in challenging conditions in broad sunlight with certain areas in shadows. The case study is therefore a good example of how the camera performs in remote areas at longer range and under more unfavourable conditions.

Extracted data: example

Despite the fact that some sub-areas are poorly matched and the extracted elevation model lacks a complete areal coverage, the handheld camera based mapping/elevation extraction

approach provides some interesting possibilities. This is particular the case considering the simplicity and low cost involved in the data collection under challenging conditions.

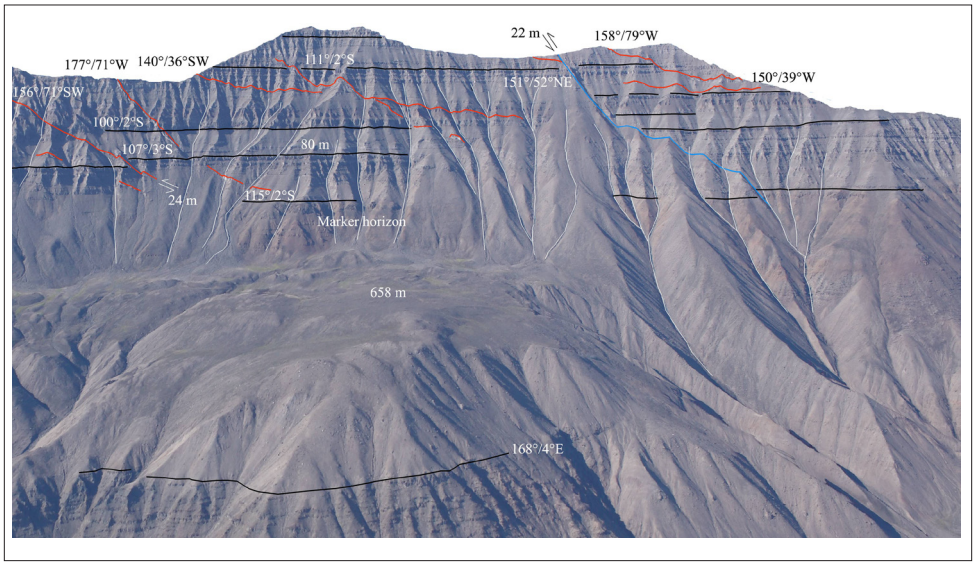

Figure 9 - Example of a DOM combining results from stereoscopic 3D-feature mapping and extracted elevation data for visualization purposes. Black lines trace lava bedding while white lines trace gullies, and red lines correspond to faults which in some cases are coincident with minor fault movement. Field of view in the lower part is roughly 1800 m and in the upper part around 3000 m. Vertical relief is around 1100 m and the variation in depth amounts to around 2300 m.

The extracted data is for example well suited for visualization and mapping purposes. This is shown in figure 9 that illustrates how stereoscopic 3D-feature mapping is combined with the extracted elevation data in a simple DOM. Tracing of lava flows shows that they dip gently towards the south within the investigated section. Also evident is the presence of both gently and steeply dipping dykes that in a few cases coincide with minor fault offset. Whereas the "layer cake" stacking of lava flows is clearly marked in the elevation data in the steeper part of the outcrop, an important marker horizon in the central part above the plateau is mainly identified based on colour texture. This illustrates the importance of having both colour texture as well as elevation data in the geological interpretation. Considering the gently dipping nature of the lava flows, one possibility would be to study the entire length of the 120 km cliff section collected during the reconnaissance flight. With the present setup, manual measuring of control points along the length of the section for georeferencing would be quite time consuming. This is at present a weakness of the method but should be weighted against the high cost of acquiring a new proper aerial survey. Nevertheless, deploying ground control from aerial photographs at the same time also makes the method flexible, in the sense that an area can be surveyed without prior information, except that aerotriangulated aerial photographs must exist. However, with the advances in digital photogrammetry many of the original time consuming manual tasks, such as tie-point measurement, have been replaced

by automatic processes, which have greatly reduced the time involved. This has mainly left the control point measurement as the remaining time consuming factor for the digital photogrammetry approach. However, development of low-cost 3d motion sensors (inertial measurement unit + global positioning system) as for example used in the navigation of Unmanned Aerial Vehicle is likely to change this, which will make it feasible to collect and study long cliff sections (e.g. 120 km cliff sections).

Using photogrammetry at close range with a helicopter

Digital photogrammetry may be applied at closer range from for example a helicopter, similar to the obliquely looking lidar systems developed for mapping of steep terrains [Vallet et al., 2004; Buckley et al., 2008b; Rittersbacher et al., 2013]. Although obliquely looking lidar systems have been successfully used for detailed mapping of inaccessible near-vertical cliffs, data collection with such systems is very expensive [Hodgetts, 2013]. By using a camera-based approach, high resolution elevation data may be delivered at a fraction of the lidar data collection cost. It is our experience with traditional photogrammetry approach that the accuracy of the bundle adjustment in image space, or the relative accuracy, is typically in the sub-pixel range (1/3 pixel size), so that the ground sampling distance essentially determines the geometric accuracy of the model. This means that for example photographing the cliff from 300 m distance using a similar camera setup would give images with a ground sampling distance and geometric accuracy of around 5.5 cm. While the expected depth accuracy would be around 13 cm when assuming a constant image overlap of 60 % and a conservative 1 pixel image matching precision By increasing the image overlap and using a multi-view stereo approach to the image matching process [James and Robson, 2012; Wenzel et al., 2013] a better precision can be achieved. Wenzel et al. [2013] quoted a typical precision of 1/3 pixel for dense multi-view stereo matching using the SURE photogrammetric software [Rothermel et al., 2012]. Changing the settings in NGATE within SocetSet allows for a given point to be determined in multiple images. Assuming that a similar automatic point matching precision of 1/3 pixel is obtainable with SocetSet, the expected depth accuracy would decrease to around 4.4 cm. Extracting a point cloud under such conditions would provide a high resolution, dense and geometrically more accurate dataset. Such a dataset could for example be used to extract near-planar geological surfaces (bedding, fractures or faults) in a semi-automatic fashion using routines originally developed for TLS derived data [Roncella and Forlani, 2005; García-Sellés et al., 2011]. The absolute positional accuracy of the point cloud would be inferior to that achieved by the obliquely looking lidar system [Vallet et al., 2004; Buckley et al., 2008b]. However for many geological problems it is of less importance to have sub-metre absolute positional accuracy. This is especially so in for example outcrop-based analogue studies. If higher absolute positional accuracy is needed using oblique photogrammetry, surveyed grade GPS and IMU systems could be deployed. This would however increase the data collection cost and reduce the flexibility and simplicity of using just a hand-held camera.

Conclusion

The present study shows that detailed terrain models of geological outcrops can be generated using stereo-images acquired with calibrated handheld high-resolution digital cameras across scales and accessibility.

When compared to elevation models derived from TLS data at close range (< 120 m) only a minor difference of 0.02 - 0.09 m is observed between the two data sets. Because millimetre to centimetre scale is not needed for most geological purposes, terrestrial photogrammetry using high resolution digital cameras can in many cases be used as an alternative or supplement to a terrestrial laser scanner depending on the nature of the outcrop.
This study furthermore shows that a handheld camera can be used from a helicopter to survey a 12 km cliff section from a distance of 2-5 km within 6 min of helicopter flying time. The produced DEM is of superior resolution to elevation data extracted from existing black and white aerial photographs at the scale 1:150.000 and comparable in resolution to a DEM extracted from high-resolution (0.5 m GSD) coloured aerial photographs. DEM comparison between the newly derived dataset and the DEM extracted from conventional high resolution aerial photographs show that there is an overall good fit between the two datasets (RMSE= 6.0 m).

Acknowledgements

The authors acknowledge Geocenter Denmark, and DONG Energy for financial support of the project. Also acknowledged, is the Geomodels Research Institute, and the projects CGL2010-21968-C02-01/BTE (INTECTOSAL), CGL2010-18609 (NUTESA) from the Spanish Ministry of Science and Technology. We thank K.S. Dueholm and L.M. Larsen for thoughtful comments on the manuscript as well as two anonymous reviewers for their constructive critique. The paper is published with permission of the Geological Survey of Denmark and Greenland.

References

Ahlgren S., Holmlund J. (2003) - *Using 3-D Outcrop Laserscans for Fracture Analysis*. American Association of Petroleum Geologists, Search and Discovery, article 40099.

Asgaard U. (1968) - *Brachiopod Palaeoecology in Middle Danian Limestones at Faxe, Denmark*. Lethaia, 1 (2): 103-121. doi: http://dx.doi.org/10.1111/j.1502-3931.1968.tb01731.x.

BAE Systems (2007) - *Next-Generation Automatic Terrain Extraction (NGATE). Innovation in the cost-effective derivation of elevation data from imagery [White paper]*. Available online at: http://www.socetgxp.com/docs/education/white_papers/wp_nga te.pdf

Bellian J.A., Kerans C., Jennette D.C. (2005) - *Digital Outcrop Models: Applications of Terrestrial Scanning Lidar Technology in Stratigraphic Modeling*. Journal of Sedimentary Research, 75 (2): 166-176. doi: http://dx.doi.org/10.2110/jsr.2005.013.

Bernecker M., Weidlich O. (1990) - *The Danian (Paleocene) coral limestone of Fakse, Denmark: A model for ancient aphotic, azooxanthellate coral mounds*. Facies, 22 (1): 103-137. doi: http://dx.doi.org/10.1007/BF02536947.

Besl P.J., McKay N.D. (1992) - *A Method for Registration of 3-D Shapes*. IEEE Transactions on Pattern Analysis and Machine Intelligence, 14: 239-256. doi: http://dx.doi.org/10.1109/34.121791.

Buckley S.J., Howell J.A., Enge H.D., Kurz T.H. (2008a) - *Terrestrial laser scanning in geology: data acquisition, processing and accuracy considerations*. Journal of the Geological Society, 165 (3): 625-638. doi: http://dx.doi.org/10.1144/0016-76492007-100.

Buckley S.J., Vallet J., Braathen A., Wheeler W. (2008b) - *Oblique Helicopter-based*

laser scanning for digital terrain modelling and visualisation of Geological Outcrops. International Archives of Photogrammetry, Remote Sensing and Spatial Information Sciences, XXXVII (B4): 493-498.

Buckley S.J., Enge H.D., Carlsson C., Howell J.A. (2010) - *Terrestrial laser scanning for use in virtual outcrop geology.* The Photogrammetric Record, 25 (131): 225-239. doi: http://dx.doi.org/10.1111/j.1477-9730.2010.00585.x.

Chandler J., Ashmore P., Paola C., Gooch M., Varkaris F. (2002) - *Monitoring River-Channel Change Using Terrestrial Oblique Digital Imagery and Automated Digital Photogrammetry*. Annals of the Association of American Geographers, 92 (4): 631-644.

Dam G., Pedersen G.K., Sønderholm M., Midtgaard H.H., Larsen L.M., Nohr-Hansen H., Pedersen A.K. (2009) - *Lithostratigraphy of the Cretaceous-Paleocene Nuussuaq Group, Nuussuaq Basin, West Greenland*. Geological Survey of Denmark and Greenland Bulletin, 19, pp 171.

Dueholm K.S. (1992) - *Geologic photogrammetry using standard small-frame cameras*. Rapport Grønlands Geologiske Undersøgelse, 156: 7-17.

Dueholm K.S., Olsen T. (1993) - *Reservoir analog studies using multimodel photogrammetry; a new tool for the petroleum industry*. AAPG Bulletin, 77 (12): 2023-2031. doi: http://dx.doi.org/10.1306/BDFF8FBA-1718-11D7-8645000102C1865D.

Enge H.D., Buckley S.J., Rotevatn A., Howell J.A. (2007) - *From outcrop to reservoir simulation model: Workflow and procedures*. Geosphere, 3 (6): 469-490. doi: http://dx.doi.org/10.1130/GES00099.1.

Fabuel-Perez I., Hodgetts D., Redfern J. (2010) - *Integration of digital outcrop models (DOMs) and high resolution sedimentology - workflow and implications for geological modelling: Oukaimeden Sandstone Formation, High Atlas (Morocco)*. Petroleum Geoscience, 16 (2): 133-154. doi: http://dx.doi.org/10.1144/1354-079309-820.

Favalli M., Fornaciai A., Isola I., Tarquini S., Nannipieri L. (2012) - *Multiview 3D reconstruction in geosciences*. Computers & Geosciences, 44: 168-176. doi: http://dx.doi.org/10.1016/j.cageo.2011.09.012.

Floris S. (1980) - *The coral banks of the Danian of Denmark*. Acta Palaeontologica Polonica, 25: 531-540.

Fonstad M.A., Dietrich J.T., Courville B.C., Jensen J.L., Carbonneau P.E. (2013) - *Topographic structure from motion: a new development in photogrammetric measurement*. Earth Surface Processes and Landforms, 38 (4): 421-430. doi:1 http://dx.doi.org/10.1002/esp.3366.

García-Sellés D., Falivene O., Arbués P., Gratacos O., Tavani S., Muñoz J.A. (2011) - *Supervised identification and reconstruction of near-planar geological surfaces from terrestrial laser scanning*. Computers & Geosciences, 37 (10): 1584-1594. doi: http://dx.doi.org/10.1016/j.cageo.2011.03.007.

Garde A.A. (1992a) - *Close-range geological photogrammetry studies: field and laboratory procedures with examples from prograde granulite facies orthogneisses, Kerala, South India*. Rapport Grønlands Geologiske Undersøgelse, 156: 53-62.

Garde A.A. (1992b) - *Interpretation of flat-lying Precambrian structure by geological photogrammetry along a 65 km coastal profile in Nuussuaq, West Greenland*. Rapport Grønlands Geologiske Undersøgelse, 156: 35-40.

Gessner K., Deckert H., Drews M. (2009) - *3D visualization and analysis of fractured rock*

using digital photogrammetry. Journal of Geochemical Exploration, 101 (1): 38. doi: http://dx.doi.org/10.1016/j.gexplo.2008.11.025.

Haneberg W. (2008) - *Using close range terrestrial digital photogrammetry for 3-D rock slope modeling and discontinuity mapping in the United States*. Bulletin of Engineering Geology and the Environment, 67 (4): 457-469. doi: http://dx.doi.org/10.1007/s10064-008-0157-y.

Hirschmüller H. (2005) - *Accurate and Efficient Stereo Processing by Semi-Global Matching and Mutual Information.* IEEE Conference on Computer Vision and Pattern Recognition (CVPR), San Diego, CA, USA, June 20-26, 2005. doi: http://dx.doi.org/10.1109/cvpr.2005.56.

Hodgetts D. (2013) - *Laser scanning and digital outcrop geology in the petroleum industry: A review*, Marine and Petroleum Geology, 46: 335-354. doi: http://dx.doi.org/10.1016/j.marpetgeo.2013.02.014.

Jaboyedoff M., Metzger R., Oppikofer T., Couture R., Derron M.-H., Locat J., Turmel D. (2007) - *New insight techniques to analyze rock-slope relief using DEM and 3D-imaging cloud points: COLTOP-3D software*. In: Eberhardt E., Stead D., Morrison T. Rock mechanics: Meeting Society's Challenges and demands, 2, Taylor Francis: 61-68. doi: http://dx.doi.org/10.1201/noe0415444019-c8.

James M., Robson S., Pinkerton H., Ball M. (2006) - *Oblique photogrammetry with visible and thermal images of active lava flows*. Bulletin of Volcanology, 69 (1): 105-108. doi: http://dx.doi.org/10.1007/s00445-006-0062-9.

James M.R., Pinkerton H., Robson S. (2007) - *Image-based measurement of flux variation in distal regions of active lava flows*. Geochemistry, Geophysics, Geosystems, 8 (3), Q03006. doi: http://dx.doi.org/10.1029/2006GC001448.

James M.R., Robson S. (2012) - *Straightforward reconstruction of 3D surfaces and topography with a camera: Accuracy and geoscience application*. Journal of Geophysical Research, 117 (F3), F03017. doi: http://dx.doi.org/10.1029/2011JF002289.

Janson X., Kerans C., Bellian J.A., Fitchen W. (2007) - *Three-dimensional geological and synthetic seismic model of Early Permian redeposited basinal carbonate deposits, Victorio Canyon, west Texas*. AAPG Bulletin, 91 (10): 1405-1436. doi: http://dx.doi.org/10.1306/05210705188.

Kuhn D., Prüfer S. (2014) - *Coastal cliff monitoring and analysis of mass wasting processes with the application of terrestrial laser scanning: A case study of Rügen, Germany*. Geomorphology, 213: 153-165. doi: http://dx.doi.org/10.1016/j.geomorph.2014.01.005.

Lague D., Brodu N., Leroux J. (2013) - *Accurate 3D comparison of complex topography with terrestrial laser scanner: application to the Rangitikei canyon (N-Z)*. Geophysics. Retrieved from http://arxiv.org/abs/1302.1183. doi: http://dx.doi.org/10.1016/j.isprsjprs.2013.04.009.

Larsen L.M., Pedersen A.K. (2009) - *Petrology of the Paleocene Picrites and Flood Basalts on Disko and Nuussuaq, West Greenland*. Journal of Petrology, 50 (9): 1667-1711. doi: http://dx.doi.org/10.1093/petrology/egp048.

Lim M., Petley D.N., Rosser N.J., Allison R.J., Long A.J., Pybus D. (2005) - *Combined Digital Photogrammetry and Time-of-Flight Laser Scanning for Monitoring Cliff Evolution*. The Photogrammetric Record, 20 (110): 109-129. doi: http://dx.doi.

org/10.1111/j.1477-9730.2005.00315.x.

Lowe D. (2004) - *Distinctive Image Features from Scale-Invariant Keypoints*. International Journal of Computer Vision, 60: 91-110. doi: http://dx.doi.org/10.1023/B:VISI.0000029664.99615.94.

McCaffrey K.J.W., Hodgetts D., Howell J., Hunt D., Imber J., Jones R.R., Tomasso M., Thurmond J., Viseur S. (2010) - *Virtual fieldtrips for petroleum geoscientists*. Petroleum Geology Conference series, 7: 19-26. doi: http://dx.doi.org/10.1144/0070019.

Olariu M.I., Ferguson J.F., Aiken C.L.V., Xu X. (2008) - *Outcrop fracture characterization using terrestrial laser scanners: Deep-water Jackfork sandstone at Big Rock Quarry, Arkansas*. Geosphere, 4 (1): 247-259. doi: http://dx.doi.org/10.1130/GES00139.1.

Pedersen A.K., Dueholm K.S. (1992) - *New methods for the geological analysis of Tertiary volcanic formations on Nuussuaq and Disko, central West Greenland, using multi-model photogrammetry*. Rapport Grønlands Geologiske Undersøgelse, 156: 19-34.

Pedersen A.K., Larsen L.M., Riisager P., Dueholm K.S. (2002) - *Rates of volcanic deposition, facies changes and movements in a dynamic basin: the Nuussuaq Basin, West Greenland, around the C27n-C26r transition*. Geological Society, London, Special Publications, 197 (1): 157-181. doi: http://dx.doi.org/10.1144/GSL.SP.2002.197.01.07.

Pedersen A.K., Larsen L.M., Pedersen G.K., Dueholm K.S. (2006) - *Five slices through the Nuussuaq Basin, West Greenland*. Geological Survey of Denmark and Greenland Bulletin, 10: 53-56.

Pedersen G.K., Larsen L.M., Pedersen A.K., Hjortkjær B.F. (1998) - *The syn-volcanic Naajaat lake, Paleocene of West Greenland*. Palaeogeography, Palaeoclimatology, Palaeoecology, 140 (1-4): 271-287. doi: http://dx.doi.org/10.1016/S0031-0182(98)00034-0.

Pringle J.K., Westerman A.R., Clark J.D., Drinkwater N.J., Gardiner A.R. (2004) - *3D high-resolution digital models of outcrop analogue study sites to constrain reservoir model uncertainty: an example from Alport Castles, Derbyshire, UK*. Petroleum Geoscience, 10 (4): 343-352. doi: http://dx.doi.org/10.1144/1354-079303-617.

Rittersbacher A., Buckley S.J., Howell J.A., Hampson G.J., Vallet J. (2013) - *Helicopter-based laser scanning: a method for quantitative analysis of large-scale sedimentary architecture*. Geological Society, London, Special Publications, 387. doi: http://dx.doi.org/10.1144/SP387.3.

Roncella R., Forlani G. (2005) - *Extraction of planar patches from point clouds to retrieve dip and dip direction of rock discontinuities*. Proceedings of the ISPRS Workshop Laser scanning 2005, ISPRS Archives, Volume XXXVI, Netherlands: 162-167.

Rosser N.J., Petley D.N., Lim M., Dunning S.A., Allison R.J. (2005) - *Terrestrial laser scanning for monitoring the process of hard rock coastal cliff erosion*. Quarterly Journal of Engineering Geology and Hydrogeology, 38 (4): 363-375. doi: http://dx.doi.org/10.1144/1470-9236/05-008.

Rotevatn A., Buckley S.J., Howell J.A., Fossen H. (2009) - *Overlapping faults and their effect on fluid flow in different reservoir types: A LIDAR-based outcrop modeling and flow simulation study*. AAPG Bulletin, 93 (3): 407-427. doi: http://dx.doi.org/10.1306/09300807092.

Rothermel M., Wenzel K., Fritsch D., Haala N. (2012) - *Sure: Photogrammetric Surface Reconstruction from imagery*. Proceedings LCD3D Workshop, Berlin, December 2012.

Sagy A., Brodsky E.E., Axen G.J. (2007) - *Evolution of fault-surface roughness with slip*.

Geology, 35 (3): 283-286. doi: http://dx.doi.org/10.1130/G23235A.1.

Snavely N., Seitz S., Szeliski R. (2008) - *Modeling the World from Internet Photo Collections*. International Journal of Computer Vision, 80: 189-210. doi: http://dx.doi.org/10.1007/s11263-007-0107-3.

Sturzenegger M., Stead D. (2009) - *Close-range terrestrial digital photogrammetry and terrestrial laser scanning for discontinuity characterization on rock cuts*. Engineering Geology, 106 (3-4): 163-182. doi: http://dx.doi.org/10.1016/j.enggeo.2009.03.004.

Vallet J., Skaloud J. (2004) - *Development and experiments with a fully-digital handheld mapping system operated from a helicopter.* International Archives of Photogrammetry, Remote Sensing and Spatial Information Sciences, XXXV (B5): 791-797.

Wenzel K., Rothermel M., Fritsch D., Haala N. (2013) - *Image Acquisition and Model Selection for Multi-View Stereo*. International Archives of Photogrammetry Remote Sensing and Spatial Information Sciences, XL-5/W1: 251-258. doi: http://dx.doi.org/10.5194/isprsarchives-XL-5-W1-251-2013.

Vosgerau H., Guarnieri P., Weibel R., Larsen M., Dennehy C., Sørensen E.V, Knudsen C. (2010) - *Study of a Palaogene intrabsaltic sedimentary unit in southern East Greenland: from 3-D photogeology to micropetrography*. Geological Survey of Denmark and Greenland Bulletin, 20: 75-78.